Trend Analysis of Onboard Calibration Data of Terra/ASTER/VNIR and One of the Suspected Causes of Sensitivity Degradation

Kohei Arai *arai@is.saga-u.ac.jp*
Information Science Department
Saga University
Saga City, 840-8502, Japan

Nagamitsu Ohgi *nohgi@jaros.or.jp*
Japan Resources Observation System and Space Utilization Organization,
2-24-2 Nichibei Bldg, Hacchobori, Chuo, Tokyo, 104-0032 Japan

Fumihiro Sakuma *sakuma@jaros.or.jp*
Japan Resources Observation System and Space Utilization Organization,
2-24-2 Nichibei Bldg, Hacchobori, Chuo, Tokyo, 104-0032 Japan

Masakuni Kikuchi *kikuchi@jaros.or.jp*
Japan Resources Observation System and Space Utilization Organization,
2-24-2 Nichibei Bldg, Hacchobori, Chuo, Tokyo, 104-0032 Japan

Satoshi Tsuchida *s.tsuchida@aist.go.jp*
Advanced Industrial Science and Engineering,
1-1-1 Umezono, Tsukuba, Ibaraki 305-8568 Japan

Hitomi Inada *hinada@bx.jp.nec.com*
NEC Corporation,
1-10 Nisshin, Fuchu, Tokyo 183-8501 Japan

Abstract

Sensitivity degradation trend is analyzed for ASTER: Advanced Spaceborne Thermal Emission and Reflection radiometer/Visible and Near-Infrared Radiometer: VNIR onboard Terra satellite. Fault Tree Analysis is made for sensitivity degradation. Firstly, it is confirmed that the VNIR detectors are stable enough through dark current and shot noise behavior analysis. Then it is also confirmed that radiance of calibration lamp equipped VNIR is stable enough through lamp monitor of photodiode output data analysis. It is confirmed that radiance at the front of VNIR optics is, on the other hand, degraded in conjunction with sensitivity degradation of VNIR through an analysis of another photodiode output data which is equipped at the front of VNIR optics, photodiode output is scale-off at around one year after the launch though. VNIR optics transparency might not be so degraded due to the fact that VNIR output and the later photodiode output show almost same degradations. Consequently, it may say that one of possible causes of VNIR sensitivity degradation is thruster plume.

Keywords: ASTER, Onboard Calibration, Vicarious Calibration, Plume Impingement.

1. INTRODUCTION

Almost all the solar reflection channels of mission instruments onboard Earth observation satellite carry their own calibration system to maintain consistency of the radiometric fidelity of the instrument. Thus users may convert from the Digital Number, DN to radiance taking the onboard calibration system derived calibration coefficient into account. There are some reports on the calibration issues which include the MOS-1: Marine Observation Satellite-1[1], Landsat-7 ETM+: Enhanced Thematic Mapper Plus[2], SeaWiFS: Sea-viewing Wide Field-of-view Sensor[3],

SPOT-1 and 2: Satellite Pour l'Observation de la Terre[4], Hyperion[5], and POLDER: POLarization and Directionality of the Earth's Reflectance[6]. Onboard calibrators cannot provide results of a higher accuracy than the preflight laboratory calibration. This means that the accuracy of the in-flight (absolute) calibration is inferior to the preflight results. This is because the preflight calibration source is used to calibrate the onboard calibrators. In addition, the uncertainty of the onboard calibrator typically increases with time. Hence, it makes good sense to include additional calibration approaches that are independent of the preflight calibration. Besides the normal and expected degradation of the onboard calibrators, they also run the risk of failing or operating improperly. Therefore, vicarious approaches are employed to provide further checks on the sensor's radiometric behavior. Any electro-optical sensor is expected to degrade once in orbit, and therefore requires a mechanism to monitor the data's radiometric quality over time. Many sensors, including ASTER: Advanced Spaceborne Thermal Emission and Reflection radiometer, employ onboard calibration devices to evaluate temporal changes in the sensor responses. Onboard calibrators, in general, provide excellent temporal sampling of the sensor's radiometric behavior over time. In addition, the repeatability and precision of the onboard systems allow use of these data in characterizing the sensor's response trends. Typical approaches for onboard calibration include lamp-based, diffuser-based, and detector-based methods. ASTER VNIR: Visible and Near-Infrared Radiometer and SWIR: Short Wave Infrared Radiometer use lamp based onboard calibrators. The specific design of the ASTER OBC: Onboard Calibrator is described in the following section. Then the sensor's response trends and suspected influence due to plume impingement of contamination of optics entrance of ASTER instrument is followed by with some evidences. Finally, discussions and concluding remarks are described.

2. ONBOARD CALIBRATION SYSTEM OF TERRA/ASTER/VNIR

2.1 Onboard Calibration System

ASTER VNIR and SWIR channels use lamp-based onboard calibrators for monitoring temporal changes in the sensor responses. Space restrictions aboard the Terra platform disallow a solarbased calibration, and therefore, onboard calibration is lamp-based. The VNIR and SWIR have two onboard calibration lamps, lamp-A and lamp-B. Both are used periodically, and as a backup system. The VNIR calibration lamp output is monitored by a silicon photo monitor, and is guided to the calibration optics. The calibration optics output illuminates a portion of the VNIR aperture's observation optics and is monitored by a similar photo monitor. Meanwhile, the SWIR calibration assembly does not have a second silicon photo monitor. In the pre-flight phase, the onboard calibrators were well characterized with integration spheres calibrated with fixed freezing point blackbodies of Zn (419.5K). This was accomplished by comparing the VNIR and SWIR output derived from the integration sphere's illumination of the two sensors. The same comparison was made by the calibration lamp's (A and B) illumination of the two sensors. Next, the pre-flight gain and offset data (no illumination) were determined. In addition, MTF: Modulation Transfer Function was measured with slit light from a collimator while stray light effect was measured with the integration sphere illumination, which is blocked at the full aperture of the VNIR and SWIR observation optics entrance. The pre-flight calibration data also includes

(1) spectral response,
(2) out-of-band response.

The VNIR has two onboard calibration halogen lamps (A and B) as is shown in Figure1. The light from these lamps is led to the VNIR optics via a set of calibration optics. Filters and photomonitors are located fore and aft of the calibration optics to monitor the output of the lamps as well as any possible degradation in the calibration optics. Lamp output and photo monitor data are collected every 33 days (primarily it was 16 days of the Terra orbital revisit cycle plus one day = 17 days and is 49 days now a day), and RCC: Radiometric Calibration Coefficients are calculated from the VNIR output taking into account the photo-monitor output. The RCC values are normalized by the pre-flight data to determine their final estimate. This procedure is the same for the SWIR RCC calculation except that the SWIR OBC does include a photo monitor system at the lamp but does not include a photo monitor system for entrance of the optics. Thus, only data

from a photo monitor that is aft of the calibration lamp is taken into account.

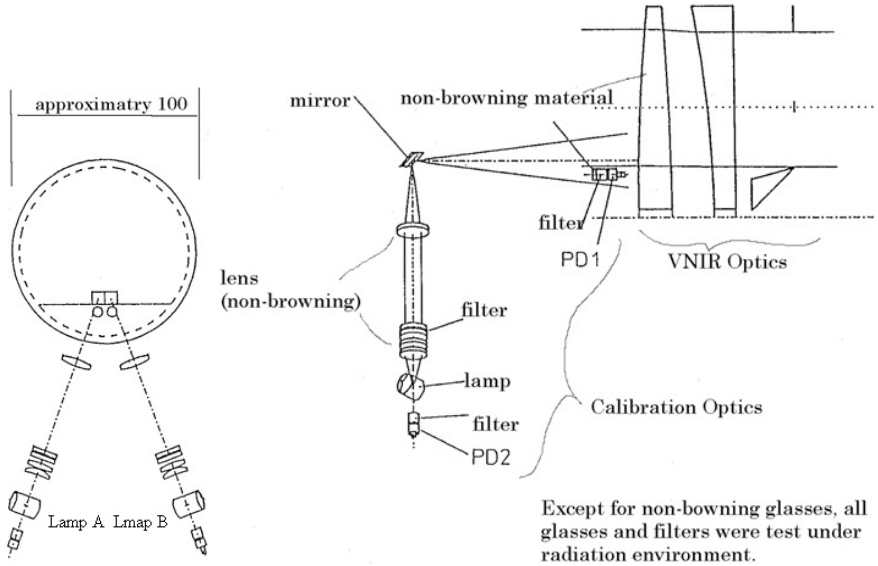

FIGURE 1: Onboard calibration system of the ASTER/VNIR

2.2 Onboard Calibration Trend

Figure2 shows the RCC trends for VNIR.

OBC RCC

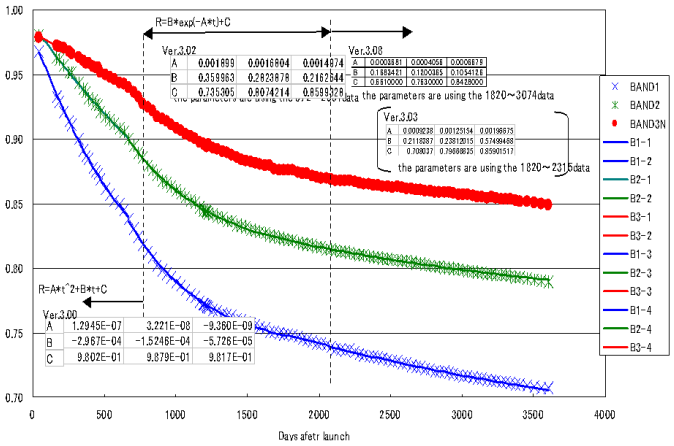

FIGURE 2: OBC RCC trends for Band 1(Blue), Band 2(Green) and Band 3(Red)

The RCC were changed relatively rapidly in the early stage of the launch, and is changed gradually for the time being. These are approximated with an exponential function with a bias and a negative coefficient. If the trend is approximated with the function of RCC = B exp (-At) + C, then A, B, and C equal the following values: Band1 (560nm): A = 0.00190, B = 0.360, C = 0.735 Band2 (660nm): A = 0.00168, B = 0.282, C = 0.807Band3 (810nm): A = 0.00150, B = 0.216, C = 0.860 During 2500 days after the launch, VNIR OBC RCC were degraded about 10% for Band3, 16% for Band2 and 23 % for Band1, respectively while SWIR OBC RCC were degraded approximately 2.0 to 3.5% depending on bands[7]. These trends are very similar to the vicarious calibration derived RCC, and also look similar to the OBC RCC trend of the OPS: Optical Sensor onboard the JERS-1: Japanese Earth Resources Satellite, a legacy precursor to the ASTER instrument. There are two major trends in OBC RCC trends, at the first 800 days and at the 2100

days after the launch as is shown in Figure2. It is suspected that out-gas from the materials of VNIR instrument and thruster plume in the initial phase. Each of the VNIR bands is shown, as are the onboard calibrator results for these bands in a fashion similar to that shown in Figure 2. On the other hand, Figure 3 shows vicarious calibration trend [8]. Although both onboard and vicarious calibration trends are similar, there are small biases, a few percents for Band 1 to 3N as is indicated in Figure 3. Therefore, VNIR sensitivity degradation is confirmed with the different two sources. VNIR sensitivity degradation can be expressed with exponential function so that one of the possible causes of the degradation is contamination. The other causes are degradation of optical transparency of the calibration optics, sensitivity degradation of photo-monitor, degradation of photmonitor filter, etc.

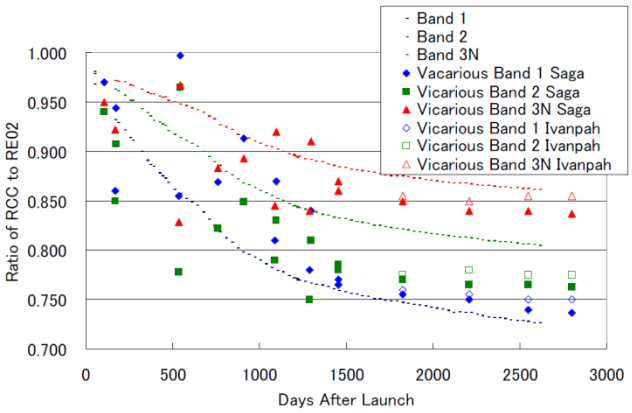

FIGURE 3: OBC and Vicarious RCC Trends

2.3 Photo-Monitor Output Trend

As is shown in Figure 1, VNIR has two photo-monitors, one (PD2) is set at lamp output and the other one (PD1) is set at the optics entrance, just in front of the collecting mirror.

Although PD1 output shows scale-off at around 370 days after launch as is shown in Figure 4, the degradation of the degradation ratio shows almost same trend as OBC and vicarious RCC trends. Also PD2 output shows stable lamp illumination so that one of possible causes for the sensitivity degradation is contamination at the optics entrance because the calibration optics is composed with browning lenses (less degradation of transparency due to radiation from solar flare). From the PD1 output data, approximated exponential function is estimated with least square method. The degradation rate is confirmed to be almost same as OBC and vicarious RCC trends as is shown in Figure 5.

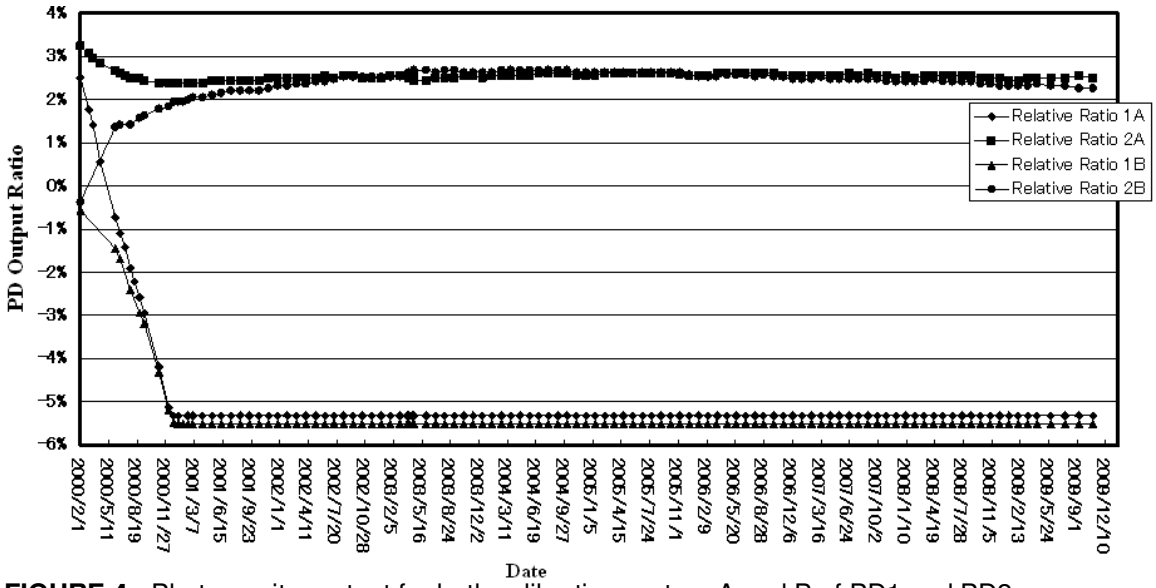

FIGURE 4 : Photomonitor output for both calibration system A and B of PD1 and PD2.

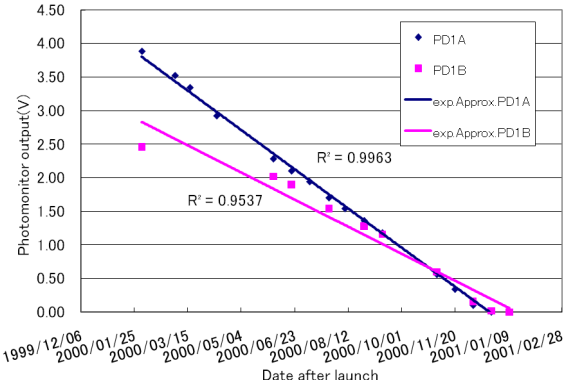

FIGURE 5 : Approximated exponential function of PD1 output using PD1 data taken in 370 days after launch together with the other photomonitor output trends.

R square for this exponential approximation for PD1A is 0.9963 so that exterpolation might be possible accurately. OBC RCC trends with reference to the calibration systems (Lamp A and B as well as photo-monitor PD1 and 2) are shown in Figure 6. In the figure, exterpolation curve is shown as “pd1a(Exterpolation)”, photomonitor output voltage shows negative for the period 370 days after launch though.

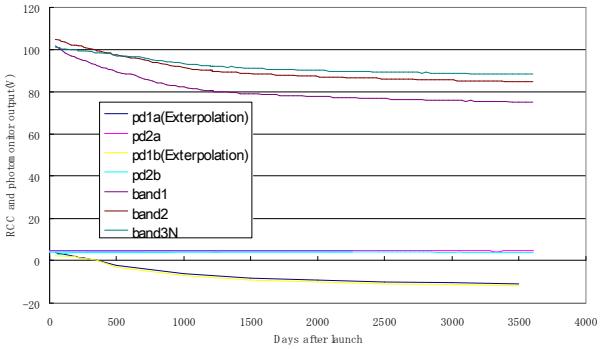

FIGURE 6 : OBC RCC trend together with photo-monitor output trend.

The first three lines are for Band 3, 2 and 1, respectively, of RCC ranges from 105 (just after the launch) to 76 at around 3600 days after launch while the last four lines are for photo-monitor output. As is mentioned before, photo-monitor PD1 for both lamp A and B were in scale off at 370 days after launch so that PD1 (lamp A and B) trend were extrapolated by the exponential function with coefficients determined from the PD1 output data of the first 370 days. As is shown in Figure 6, the coefficients of exponential function of RCC trend is almost same as that of exterpolation function of PD1. Thus it might be concluded that one of the possible causes of the RCC degradation would be contamination at the optics entrance of VNIR due to plume impingement. Thruster plume of hydrazine hydrate has not only absorption band at around 12mm but also continuous absorption in the visible region (absorption coefficient is not large though)[1]. Also hydrazine absorption in visible wavelength region is reported [9]. They measured spectral absorption of liquid as a product of hydrazine [10] with several chemicals. Consequently, they found the very calm peak absorption at around 460-480nm. For these reasons, there is a little absorption in visible wavelength region due to hydrazine hydrate of thruster plume which may affect to degradation of optics transparency of mission instruments onboard satellites.

2.4 Possible Causes of Sensitivity Degradation and Fault Tree Analysis

Firstly, it is shown that VNIR detector sensitivity is stable. As is shown in Figure 7 and 8, dark signal (Output signal when no input from the VNIR optics entrance (Night time observation)) and detector temperature is very stable so that it may say that detector sensitivity is stable enough.

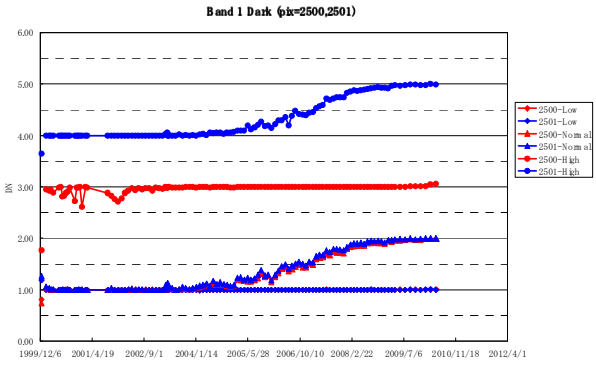

[1] http://www.coe.ou.edu/sserg/web/Results/EPA%20Spectra/N2H4%20etc.pdf

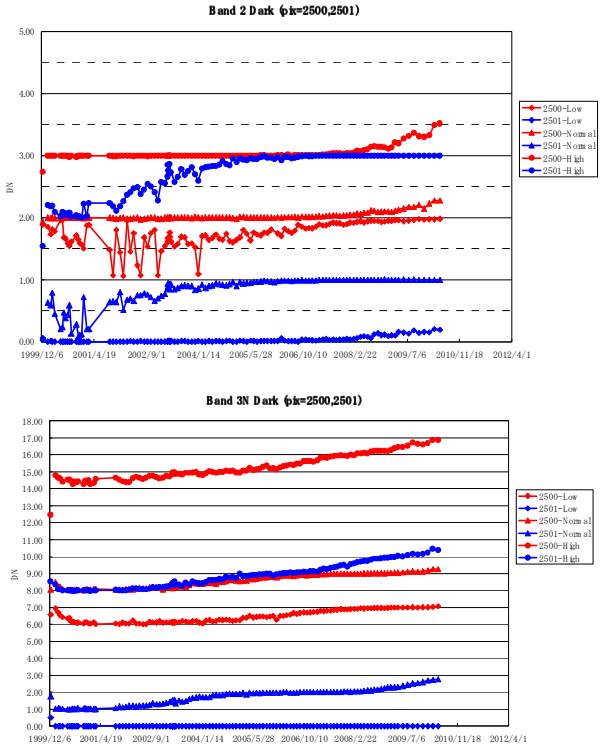

FIGURE 7: Dark signals for Bands 1(Top), 2(Middle), 3(Bottom)

FIGURE 8: Detector temperature for Bands 1,2,3.

As is shown in Figure 4, radiance from the calibration lamp is also stable so that optical transparency of VNIR optics might be degraded. There are some possible causes of the VNIR optical transparency degradation those are (1) Initial phase and (2) Long term sensitivity degradations. In the initial phase, out-gas from materials of VNIR is one of them followed by thruster plume contamination. For the long term degradation, optical transparency degradation due to ultra-violet and solar radiation as well as thruster plume is major causes. Optical transparency degradation due to ultra-violet light polymerization of optics is one of those followed by browning of optics. Fault Tree is shown in Figure 9.

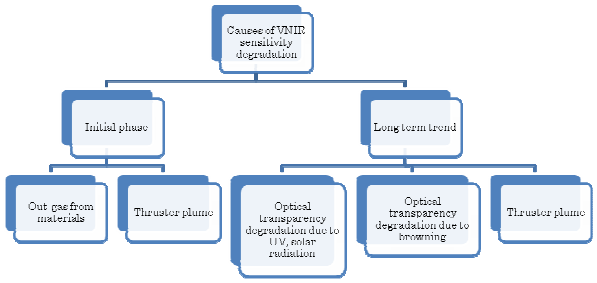

FIGURE 9: Fault Tree for VNIR sensitivity degradation

VNIR optics employs non-browning materials so that it may not occur browning in the optics. Ultra-violet light polymerization of optics might be occurred. It used to be occurred due to organic gas contamination on optics surface, in particular, coating material of the sensor optics onboard satellite[11].

Although VNIR does not employ such coating material at all, it is difficult to say it is not a cause. Thus thruster plume is one of possible causes.
During hydrazine is burning from thruster, plume includes not only hydrazine, N_2H_4, but also NH_3, H_2O, N_2, H_2. Mass fraction of N_2 is dominant followed by NH_3. Terra satellite carries two types of monopropellant of thruster, 5lbf and 1lbf. Plume impingement rate at aperture of NH_3 is dominant followed by H_2O and N_2H_4. Re-emission rate for these molecules are greater than impingement rate so that the surface of the VNIR optics is not accumulate anything. Hydrazine hydrate stick[2] on the surface of optics would occur so that it is suspected that some mixture of hydrazine such as $H_4N_2 \cdot H_2O$ is remained on the surface of VNIR optics (sticking fraction of N_2H_4 is 0.1% in accordance with the site of footnote below 2).

Although hydrazine hydrate has no absorption in visible and near infrared wavelength region, transparency in that region is not 100%. Transparency of $H_4N_2 \cdot H_2O$ is 96% at around VNIR Band 1, 97% at around Band 2 and 98% at around Band 3, respectively. This situation is much severe for short wave infrared region, SWIR. Sensitivity degradation of SWIR is not so significant and is much less than VNIR. One of the reasons for this is that thruster plume is situated in front of optics as a particle, it is not realistic though. Thus sticking hydrazine hydrate on the optics might not be a suspect so that ultra-violet light polymerization of optics might be a suspect. Further investigation is needed.

2.5 Size Distribution of Thruster Plume

From the wavelength dependency of OBC RCC trend, it is possible to estimate size distribution if it is assumed that plume impingement is one of possible causes of the RCC degradation [12],[13]. Figure 10 shows wavelength dependency of the RCC degradations. From this spectral dependency, size distribution is estimated with the assumption that the size distribution is followed by the power law as well as the accumulated number of particles is normalized by one. Figure 11 shows the estimated size distribution. The size distribution estimation has not been validated yet.

[2] http://www.gps.caltech.edu/genesis/Thrusters.html

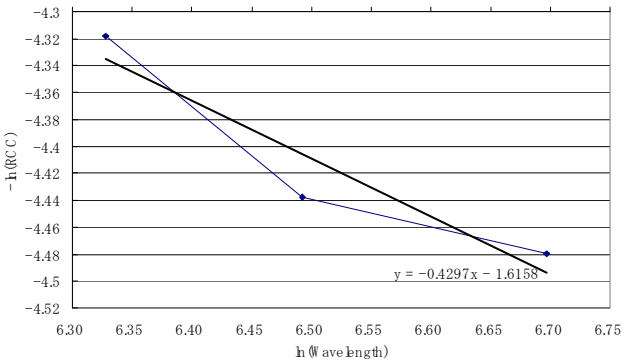

FIGURE10: Spectral characteristics of RCC and its linearly approximated function.

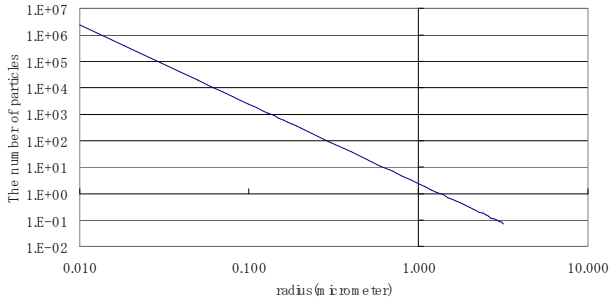

FIGURE11: Estimated size distribution of plume impingement that is one of causes of the RCC degradation

2.6 Size Distribution and SWIR Sensitivity Degradation

From Figure 11, it can be assumed that hydrazine hydrate is distributed at the optics surface sparsely because most of hydrazine hydrate particle size is smaller than 1 micrometer and the number of the particles with 0.1 micrometer of radius is around 2000 while the number of particle with 0.01 micrometer of radius is 2 million. On the other hand, SWIR sensitivity degradation for each band is around 1.2%, 2.7%, 2.7%, 2.5%, 2.4%, and 2.7% for Band 4-9 within the first 7 and half years after the launch. Meanwhile, the center wavelength of SWIR of each band is 1.65, 2.165, 2.205, 2.26, 2.33 and 2.395 micrometer for Band 4-9 so that hydrazine hydrate particles are small enough for influencing to optics transparency through scattering. It is said that hydrazine hydrate particles do not affect to the sensitivity degradation for SWIR wavelength regions.

2.7 Fuel Consumption and RCC Trend

Another evidence of the causes of RCC degradation is the relation between fuel consumption and RCC degradation. Figure 12 shows the fuel consumption of Terra satellite which carries ASTER/VNIR. Figure 12 also shows approximated function of the fuel consumption together with approximated function of RCC degradation. As is well known that the fuel consumption in just after launch is relatively large, there is bias between the two approximated functions of fuel consumption and RCC degradation. Both functions, however, show almost same trend.

Figure 13 also shows the OBC RCC trends, with the reference to the two calibration systems, Lamp A and B as well as PD2, for Band 1, 2 and 3. Figure13 also shows the fuel consumption and its approximated function with exponential function. It may say that theses show almost same trend.

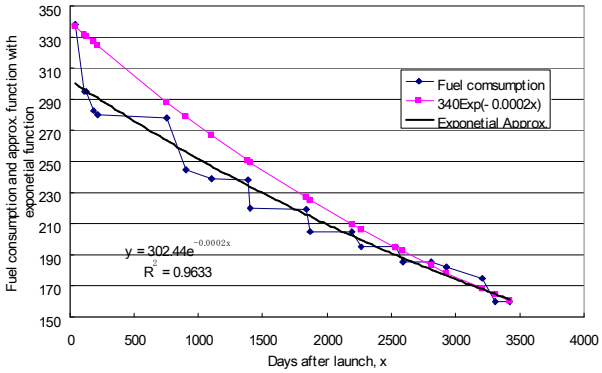

FIGURE 12: The relation between fuel consumption and RCC degradation.

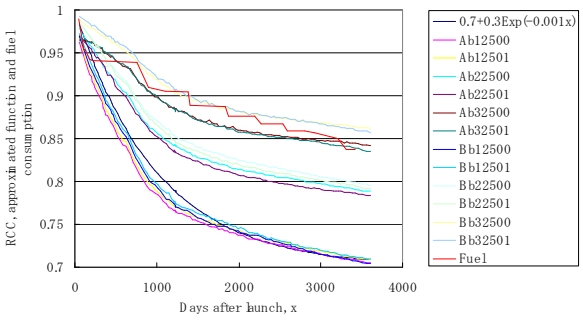

FIGURE 13: Relations between OBC RCC trend and fuel consumption as well as the approximated function of fuel consumption.

2.8 Comparison between Terra/MODIS and VNIR Sensitivity Degradations

Also sensitivity degradation of VNIR is compared to that of Terra/MODIS: Moderate Resolution Imaging Spectroradiometer because ASTER/VNIR and MODIS is onboard and their optics is equipped at Earth pointed plane on the same satellite, Terra so that almost same thruster plume influence may occur for both optics.

Sensitivity degradation of MODIS is well reported[13] so that it is compared to that of VNIR. There are three obvious epochs on around 520, 900 days and 1400 days after launch in terms of coincidence between fuel consumption and sensitivity degradation. These are common to both mission instruments, VNIR and MODIS.

Also these sensitivity degradations for both show coincident to the fuel consumption. Also according to X. Xiong et.al (2006), sensitivity degradation ratio between MODIS bands 8(412nm) and 4(554nm) as well as bands 4 and 17(905nm) are approximately 5.5 and 6.0, respectively. Meanwhile, sensitivity degradation ratio between VNIR and 1(560nm) and 3(810nm) is around 2.2. On the other hand, sensitivity degradation of MODIS band 4 is around 6% at 1500 days after launch while that of VNIR band 1 is 24%. Sensitivity degradation of VNIR is much significant than MODIS.

2.9 RCC Comparison between VNIR Band 3N and 3B

VNIR has two telescopes, band 1, 2 and 3N (Nadir looking) and band 3B (Backward looking) as is illustrated in Figure 14. Both telescope are equipped at the different location with the different angle (3N is pointing to the nadir while 3B is pointing to off-nadir with 27.6 degree). Contamination situations for both telescopes, therefore, are different. For this reason, sensitivity degradations for these two may be different. Figure 15 shows the difference between vicarious calibration data derived RCC for both. Because Band 3B does not have any onboard calibration system so that only vicarious calibration data derived RCC is discussed. If the thruster plume comes from the front of optics uniformly, then contamination of backward optics is 11.38%

(cos(27.6 degree)) less than nadir optics. Both degradations show 8.54% difference between Band 3N and Band 3B so that it is close to 11.38% of less contamination of backward telescope of Band 3B due to thruster plume.

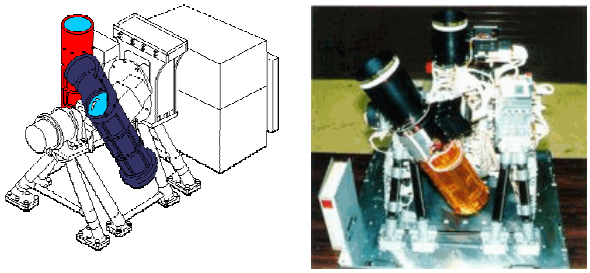

FIGURE 14: Illustrative view of VNIR instrument.

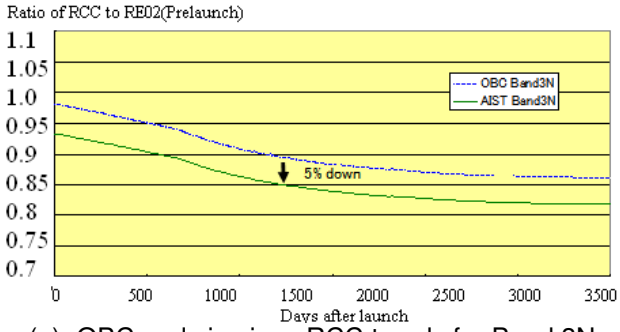

(a) OBC and vicarious RCC trends for Band 3N

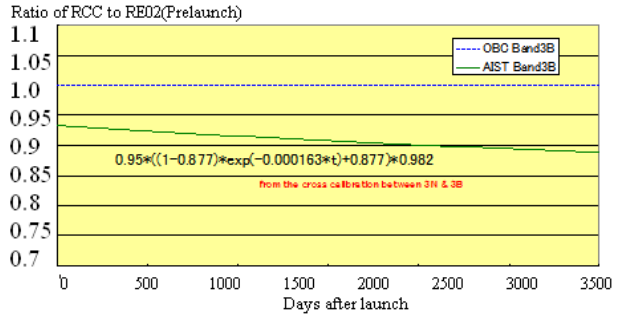

(b) Vicarious RCC trend for Band 3B

FIGURE 15: Difference of OBC RCC and vicarious calibration data derived RCC for both Band 3N and Band 3B.

Consequently, optics transparency seems to be most suspected cause of the RCC (sensitivity) degradation due to plume impingement by hydrazine hydrate from the thrusters.

2.10 Another Evidence of Contamination of ASTER/TIR Optics With Thruster Plume

ASTER composed with three mission instruments, VNIR, SWIR and Thermal Infrared Radiometer (TIR) which has five spectral channels in the atmospheric window. Sensitivity degradation of TIR Band 12 (9.1 micrometer of spectral channel) is significant followed by the Band 10, 11 as well as Band 13 and 14 as is shown in Table 1. Table 1 shows wavelength coverage and annual degradation of sensitivity.

During thruster burns hydrazine, hydrazine + water will be plumed. Hydrazine Hydrate (N2H4+H2O) has an absorption line at around 9.1μm11 so that it is understandable that sensitivity degradation is significant [15]. Also sensitivity degradation of Band 12 is much

significant in comparison to the other bands. Therefore, it is confirmed that hydrazine hydrate contaminated at the optics surface TIR as well as VNIR and SWIR.

Band No.	Wavelength
10	8.125 ~ 8.475μm
11	8.475 ~ 8.825μm
12	8.925 ~ 9.275μm
13	10.25 ~ 10.95μm
14	10.95 ~ 11.65μm

TABLE 1: Spectral channels of ASTER/TIR

3. CONCLUDING REMARKS

Due to the fact that dark signal and shot noise as well as circumstances of the VNIR such as detector temperature are stable so that detector of the VNIR is stable. Calibration lamp radiance monitor of photodiode output is stable so that calibration lamp is stable. Optics entrance monitor of photodiode which measures calibration lamp radiance shows a remarkable degradation. It was terminated 370 days after the launch, though. The degradation trend is almost same as OBC/RCC degradation (VNIR sensitivity degradation) if exterpolated degradation of optics entrance calibration radiance is compared to OBC/RCC. VNIR optics transparency is not so degraded. One of the possible causes of OBC/RCC degradation comes from contamination or ultra-violet light polymerization on the surface of VNIR optics entrance.

Assumption of which RCC degradation is caused by contamination of optics entrance of VNIR due to plume impingement from gas jet for attitude control seems to be reasonable. Sticking fraction of hydrazine is 0.1 while absorption coefficients at 500, 600, 700nm are 0.4, 0.3, 0.2%. Vicarious calibration shows difference sensitivity degradations between VNIR Band 3N and 3B. This may be caused by the fact that the optics for Band 3N is pointing to nadir while for Band 3B is pointing to 27.6 degree off-nadir because contamination situation due to thruster plume is different each other. Optics component are same for Band 3N and 3B so that both of the ultra-violet light polymerization and the sticking hydrazine hydrate are suspected. Similarly, MODIS sensitivity degradation shows a coincidence to VNIR OBC/RCC trend in terms of three obvious epochs on 520, 900 and 1400 days after the launch.

These three epochs are similar to the fuel consumption epochs. Using wavelength dependency of RCC degradation, size distribution is estimated with the relation between ln(wavelength) and ln(RCC degradation) based on power low distribution function. It has to be validated though. In a realistic case, thruster plume sticks to the optics but not situated as a particle. There is an evidence of sticking hydrazine hydrate on the TIR optics due to the fact that absorption wavelength of hydrazine hydrate corresponds to the most significant sensitivity degradation band of TIR. Consequently, optics transparency would be a most suspected cause of the RCC (sensitivity) degradation due to plume impingement by hydrazine hydrate from the thrusters or ultra-violet light polymerization of optics. Further investigation is needed.

4. REFERENCES

[1] Arai K., Preliminary assessment of radiometric accuracy for MOS-1 sensors, International Journal of Remote Sensing, 9, 1, 5-12, 1988.

[2] Barker, J.L., S.K. Dolan, et al., Landsat-7 mission and early results, SPIE, 3870, 299-311, 1999.

[3] Barnes, R.A., E.E.Eplee, et al., Changes in the radiometric sensitivity of SeaWiFS determined from lunar and solar based measurements, Applied Optics, 38, 4649-4664, 1999.

[4] Gellman, D.I., S.F. Biggar, et al., Review of SPOT-1 and 2 calibrations at White Sands from launch to the present, Proc. SPIE, Conf.No.1938, 118-125, 1993.

[5] Ungar S.G., E.M. Middleton, L. Ong, P.K.E. Campbell, EO-1 Hyperion onboard performance over eight years: Hyperion Calibration, http://eo1.gsfc.nasa.gov/new/SeniorReviewMaterial_References.doc

[6] Hagolle, O., P.Galoub, et al., Results of POLDER in-flight calibration, IEEE Trans. On Geoscience and Remote Sensing, 37, 1550-1566, 1999.

[7] Sakuma F., A.Ono, M.Kudoh, H.Inada, S.Akagi, and H.Ohmae, ASTER on-board calibration status, Proc. SPIE, 4881, 407-418, 2002.

[8] Thome, K., K. Arai, S.Tsuchida, S.Biggar, Vicarious Calibration of ASTER via Reflectance-Based Approach, IEEE Trans. on Geoscience and Remote Sensing, 46, 10, 2008.

[9] Daniela Dirtu, Lucia Odochian, Aurel Pui, Ionel Humelnicu, Thermal decomposition of ammonia. N2H4 –an intermediate reaction product, Central European Journal of Chemistry, DOI: 10.2478/ s11532-006-0030-4, 2006.

[10] During, J.R., S.F. Bush and E.E. Mercer: “Vibrational spectrum of hydrazine and a Raman study of hydrogen bonding in hydrazine”, The J. Chem. Physics”, 44, 11, 4238–4247, 1966.

[11] Itoh, N., M.Katoh, N.Okano, Comparison of spectral transmittance degradation due to organic gas contamination with on-orbit degradations of launched sensors, Proceedings of SPIE, 7149, 7149F, 2008.

[12] Arai, K., N.Ohgi, H.Inada, Suspected plume impingement onboard calibration system of Terra/ASTER investigated through trend analysis onboard calibration data, Proceedings of the ISPRS Commission VIII, WG VI/4, 2010.

[13] Kohei Arai,Nagamitsu Ohgi, Fumihiro Sakuma, Satoshi Tsuchida, Hitomi Inada, Trend analysis of onboard calibration data of Terra/ASTER/VNIR and one of the suspected causes of sensitivity degradation, Proceedings of the Conference on Characterization and Radiometric Calibration for Remote Sensing (CALCON 2010), 2010.

[14] X. Xiong, A. Wu, J. Esposito, J. Sun, N. Che, B. Guenther, W. Barnes, Trending Results of MODIS Optics On-orbit degradation , *Proceedings of SPIE Earth Observing Systems VII*,4 814, 2002.

[15] Sakuma F., M.Kikuchi, N.Ohgi, and H.Ono, ASTER TIR sensitivity degradation and hydrazine, Proceedings of the 49th General Assembly of the Remote Sensing Society of Japan, 2010.